UNIVERSITI SAINS MALAYSIA

USM

UNIVERSITI SAINS MALAYSIA

Determination Of Effective Source To Surface Distance For Electron Beam From Siemens Primus Linear Accelerator

Dissertation submitted in partial fulfillment for the Degree of Bachelor of Health Sciences (Medical Radiation)

Hong Siew Ping

School of Health Sciences
Universiti Sains Malaysia
Health Campus
16150, Kubang Kerian, Kelantan
Malaysia

2004

TITLE

Determination Of Effective Source To Surface Distance For Electron Beam From Siemens Primus Linear Accelerator

by

Heng Siew Ping

Dissertation submitted in partial fulfillment for the Degree of Bachelor of Health Science (Medical Radiation)

School of Health Sciences
Universiti Sains Malaysia
16150 Kubang Kerian Kelantan
Malaysia

2004

CERTIFICATE

This is to certify that the dissertation entitled

"Determination of effective source to surface distance for

electron beam from Siemens Primus Linear Accelerator"

is the bonafide record of research work done by

Ms Heng Siew Peng during the period of

June 2003 to January 2004 under my supervision.

Signature of Supervisor

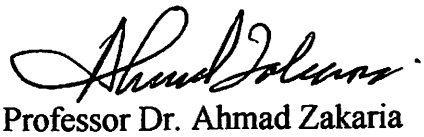

Professor Dr. Ahmad Zakaria
Department of Oncology and Radiotherapy
School of Medical Science.
Health Campus,
University Science of Malaysia
Date: 3rd April 2004

ACKNOWLEDGEMENTS

I would like to thank Professor Dr. Ahmad Zakaria and Encik Nik for many useful discussions and correcting the drafts. I also thank technical assistants Mr Nizam for willing explained and guided me about procedures involved in this research project. Lastly, I would also like to express my appreciation to various individuals, too numerous to mention individually, who provided assistance during the course of the project.

TABLE OF CONTENTS

	Page
TITLE	i
CERTIFICATE	ii
ACKNOWLEDGEMENTS	iii
TABLE OF CONTENTS	iv
LIST OF TABLES, FIGURES, GRAPHS AND ILLUSTRATION	v-viii
1. ABSTRACT	1
2. INTRODUCTION	2 – 6
3. OBJECTIVE OF STUDY	7
4. MATERIALS AND MEYHODS	8-14
5. RESULTS	15-74
6. DISCUSSION	75-77
7. CONCLUSION	78
8. REFERENCES	79-81
9. APPENDIX	

LIST OF TABLES, FIGURES, GRAPHS AND ILLUSTRATIONS

List of figures:

Figure	Title	Page
1	Isocentric mounting	5
2	Definition of effective source surface distance	6
3	30 cm x 30 cm slabs of solid water phantom	11
4	The experiment set up showing the virtual source position, effective SSD, air gap and depth of measurement	12
5	Linac and solid water phantom setup	13
6	A plot of the inverse square root of the ratio of ionization against g, with linear fits determined by regression analysis to the data for the 5 cm diameter circle and a range of beam energies, measured at d_{max}	26
7	A plot of the inverse square root of the ratio of ionization against g, with linear fits determined by regression analysis to the data for the 10 cm x 10 cm applicator and a range of beam energies, measured at d_{max}	33
8	A plot of the inverse square root of the ratio of ionization against g, with linear fits determined by regression analysis to the data for the 15 cm x 15 cm applicator and a range of beam energies, measured at d_{max}	40
9	A plot of the inverse square root of the ratio of ionization against g, with linear fits determined by regression analysis to the data for the 20 cm x 20 cm applicator and a range of beam energies, measured at d_{max}	47
10	A plot of the inverse square root of the ratio of ionization against g, with linear fits determined by regression analysis to the data for the 25 cm x 25 cm applicator and a range of beam energies,	54

	measured at d_{max}	
11	Variation of effective SSD with electron beam energy	56
12	Variation of effective SSD with applicator size for different energies	57
13	Effective SSD determined by graphical extrapolation for 6 MeV electron beam for 5 cm diameter circle	58
14	Effective SSD determined by graphical extrapolation for 6 MeV electron beam for 10 cm x 10 cm applicator	59
15	Effective SSD determined by graphical extrapolation for 6 MeV electron beam for 15 cm x 15 cm applicator	60
16	Effective SSD determined by graphical extrapolation for 6 MeV electron beam for 20 cm x 20 cm applicator	61
17	Effective SSD determined by graphical extrapolation for 6 MeV electron beam for 25 cm x 25 cm applicator	62
18	Effective SSD determined by graphical extrapolation for 9 MeV electron beam for 5 cm diameter circle	63
19	Effective SSD determined by graphical extrapolation for 9 MeV electron beam for 10 cm x 10 cm applicator	64
20	Effective SSD determined by graphical extrapolation for 9 MeV electron beam for 15 cm x 15 cm applicator	65
21	Effective SSD determined by graphical extrapolation for 9 MeV electron beam for 20 cm x 20 cm applicator	66
22	Effective SSD determined by graphical extrapolation for 9 MeV electron beam for 25 cm x 25 cm applicator	67
23	Effective SSD determined by graphical extrapolation for 15 MeV electron beam for 5 cm diameter circle	68
24	Effective SSD determined by graphical extrapolation for 9 MeV electron beam for 10 cm x 10 cm applicator	69
25	Effective SSD determined by graphical extrapolation for 9 MeV electron beam for 15 cm x 15 cm applicator	70

26	Effective SSD determined by graphical extrapolation for 9 MeV electron beam for 20 cm x 20 cm applicator	71
27	Effective SSD determined by graphical extrapolation for 9 MeV electron beam for 25 cm x 25 cm applicator	72

List of tables:

Table	Title	Page
1	Depth of maximum dose as a function of energy and field size	14
2	Measured data for 6 MeV electron energy; 5 cm diameter circle	20
3	Calculation of the total sum of squares, Sxx and Sxy	21
4	Measured data for 9 MeV electron energy; 5 cm diameter circle	22
5	Calculation of the total sum of square, Sxx and Sxy	23
6	Measured data for 15 MeV electron energy; 5 cm diameter circle	24
7	Calculation of the total sum of squares, Sxx and Sxy	25
8	Measured data for 6 MeV electron energy; 10 x 10 cm^2 field size	27
9	Calculation of total sum of squares, Sxx and Sxy	28
10	Measured data for 9 MeV electron energy; 10 x 10 cm^2 field size	29
11	Calculation of the total sum of square, Sxx and Sxy	30
12	Measured data for 15 MeV electron energy; 10 x 10 cm^2 field size	31
13	Calculation of the total sum of square, Sxx and Sxy	32
14	Measured data for 6 MeV electron energy; 15 x 15 cm^2 field size	34
15	Calculation of the total sum of square, Sxx and Sxy	35
16	Measured data for 9 MeV electron energy, 15 x 15 cm^2 field size	36
17	Calculation of the total sum of square, Sxx and Sxy	37
18	Measured data for 15 MeV electron energy, 15 x 15 cm^2 field size	38
19	Calculation of the total sum of square, Sxx and Sxy	39
20	Measured data for 6 MeV electron energy, 20x 20cm^2 field size	41
21	Calculation of the total sum of square, Sxx and Sxy	42
22	Measured data for 9 MeV electron energy, 20 x 20 cm^2 field size	43

23	Calculation of the total sum of square, Sxx and Sxy	44
24	Measured data for 15 MeV electron energy, 20 x 20 cm^2 field size	45
25	Calculation of the total sum of square, Sxx and Sxy	46
26	Measured data for 6MeV electron energy, 25x 25cm^2 field size	48
27	Calculation of the total sum of square, Sxx and Sxy	49
28	Measured data for 9MeV electron energy, 25x 25cm^2 field size	50
29	Calculation of the total sum of square, Sxx and Sxy	51
30	Measured data for 15 MeV electron energy, 25x 25cm^2 field size	52
31	Calculation of the total sum of square, Sxx and Sxy	53
32	Dependence of effective SSD on incident energy and field size	55
33	Effective SSD determined by the inverse square slope and graphical extrapolation in cm for various beam energies and field sizes	73
34	Variation of effective SSD determined by inverse square slope method and graphical extrapolation	74

ABSTRACT

The aim of this thesis is to determine the effective source surface distance for 6, 9 and 15 MeV electron beam energies generated from Siemens Primus linear accelerator in HUSM. The effective SSD is the distance from the virtual source position to the end of the applicator. The effective SSD is known to depend on beam energy and field size. Different methods of obtaining the effective source surface distance for electron beams have been investigated. The charge measurements were performed using parallel plate ionization chamber in solid water phantom at depth of d_{max}, using 0, 5, 10 and 15cm air gap. Excel was used to present a plot of $[Q_o/Q_g]^{1/2}$ versus air gap. The variation of the effective SSD with the energy and field size of measurement was also investigated. Minimum effective SSD was 58.3 cm in small field size of 5 cm diameter circle applicator and maximum effective SSD was 98.2 cm for 25x25 cm^2 applicator, with 6 MeV energy. Effective SSDs gradually increased with field size for the same electron energy and decreased again at 25x25cm^2 for 6 and 9MeV. Effective SSDs gradually increased with the electron energies. From the results we recommended that the effective SSD should be measured for each energy and field size before clinical use.

INTRODUCTION

Treatment with electron beams is ideally executed at the standard source-to-surface distance with the patient skin surface at the isocenter for isocentritally mounted accelerators (Figure 1) for which depth–dose profiles and output factors are known. However, at times it becomes necessary to treat with nonstandard treatment distances due to either an irregular skin surface or anatomical constraints such as a shoulder during the treatment of the lateral posterior neck regions, which would obstruct treatment setup at standard SSD. The majority of nonstandard SSD treatments are at an extended SSD. In addition, extended SSD treatment can be deliberately used to obtain larger field sizes. The posterior neck region is normally treated with abutting photon and high energy electron field in order to avoid excess spinal cord dose. (D Rajasekar, N R Datta, K J Maria Das and S Ayyagari 2002)

At extended SSD treatments, air gap between the end of the electron beam applicator and the patient surface leads to a reduction of dose and an alteration in the depth dose curves. To obtain an accurate dose rate in the region of the tumor, correction for such an air gap must be applied. (B Paul Ravindran 1999) Correction to dose rate at extended SSD does not follow the inverse square law as the photon beam output does if the nominal value of SSD, 95cm is used. (Khan, 1978) This is due to the fact that the nominal SSD is often defined as the distance from the accelerator exit window to the phantom surface, while the apparent is in fact positioned not at the window but various distances downstream from the window. (ICRU 1972) It has been shown that this can be corrected for by the use of an inverse square factor based on the effective source surface distance. (Khan, 1978)

The effective SSD method described by Khan is most practical one, since it properly predicts the distance dependence of the output of clinical beams. In this method, the dose D'_{max} at an extended SSD is related to the dose maximum, Dmax at the standard SSD by the following inverse square law relationship:

$$D'max = Dmax \frac{(SSDeff + dmax)^2}{(SSDeff + g + dmax)^2}$$

where SSDeff is the effective SSD for calibration of a given collimator field size and energy, g equals the difference between extended SSD and standard SSD, and dmax is the depth of maximum dose on central axis. By using the effective SSD method, we can obtain maximum dose at an extended SSD by applying correction factor to maximum dose at the standard. The effective SSD must be first determined to relate extended SSD to standard SSD. Effective SSD can be defined as an intersection point of the backprojection along the most probable directions of electron motion at the patient surface. (Shroder-Babo P. 1983)This is illustrated in Figure 2.

Effective SSD could be obtained by two methods, namely the inverse slope method and the graphical extrapolation method. The effective SSD obtained from the measurements using the inverse slope method and extrapolation methods were found to be identical. (B Paul Ravidran 1999)

In inverse slope method, a series of charge measurements are made in a phantom with various air gaps between the applicator end and the phantom surface. If Q_0 is the ionization charge reading with zero gap and Qg is the reading with gap g, then, by plotting $[Q_0/Q_g]^{1/2}$ as a function of gap, a straight line is obtained. The effective SSD then equal to SSDeff = (1/ slope)-dmax. (Khan, 1984) Although the effective SSD is obtained from measurements at

dmax, its value does not change with depth of measurement. Depending upon beam energy, type of collimator and field size, the plot of $[Q_0/Q_g]^{1/2}$ versus g may gradually deviate from a straight line beyond a certain air gap. For small field size and low energies, the effective SSD for inverse square method of correcting output is valid only for a limited range of air gaps, up to about 15cm in most cases. (P M Ostwald and T Kron, 1996) For larger SSDs beyond the range of inverse square law applicability, a new output calibration should be obtained. (AAPM, 1991)

Alternatively, assuming that the electrons obey the inverse square law, curves can be plotted between inverse of the square of the charge due to ionization against air gap, and by graphical extrapolation the effective source surface distance could be determined. (Klevenhagen 1985, Sharma 1992).

The effective SSDs change with beam energy and are greatly influenced by the electron beam collimating system. (Ebert and Hoban 1995, Kapur *et al* 1998, Zhang *et al* 1999). Hence, in clinical practice, a table of effective SSDs as a function of energy and field size should be obtained to determine the output correction factor at extended SSD treated for individual linear accelerators.

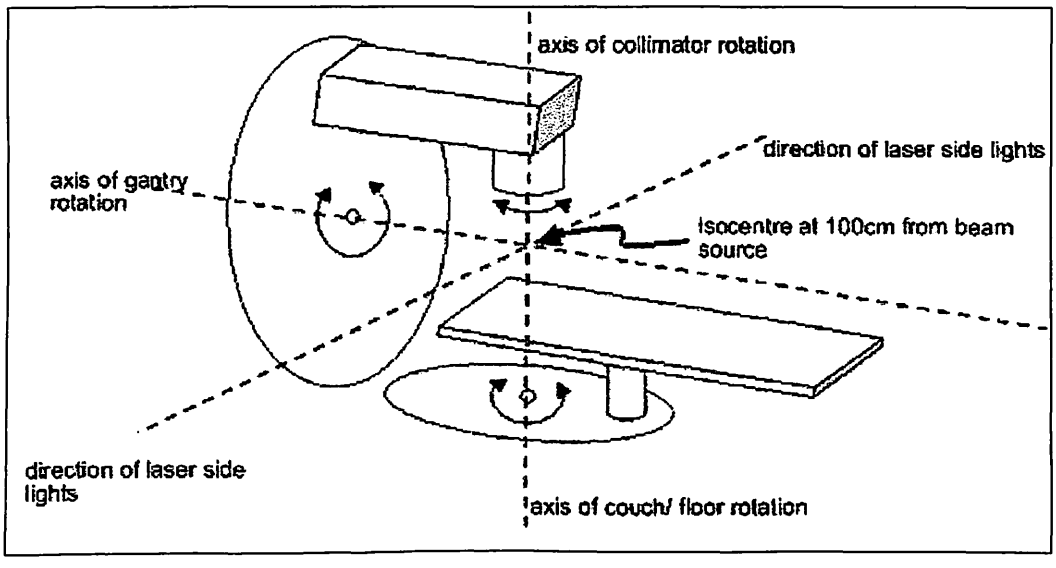

Figure 1. Isocentric mounting

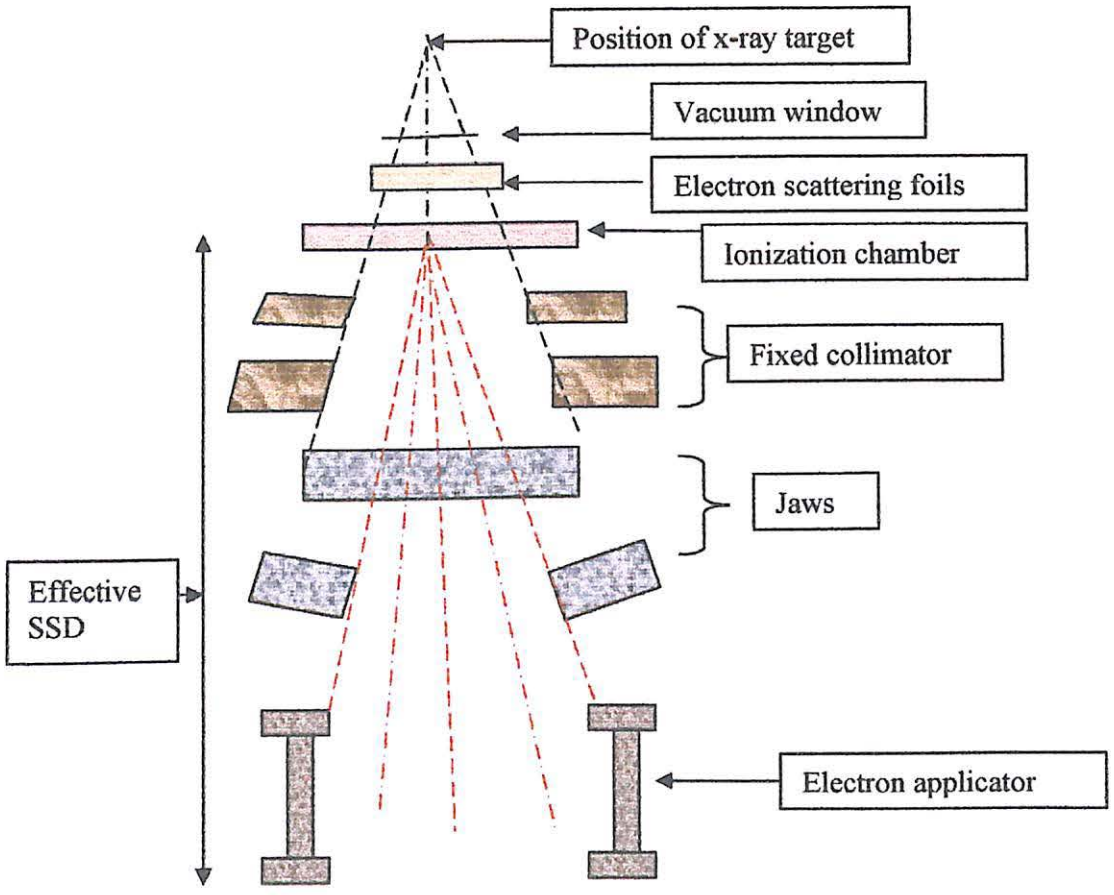

Figure 2. Definition of effective source surface distance.

OBJECTIVE

1) The purpose of this study is to determine the effective SSDs as a function of energy and field size in order to give the correct inverse square law relationships for the change in output with distance. Electron beams of energies 6, 9 and 15 MeV from a Siemens Primus linear accelerator were investigated. Insert was made for a 5cm diameter circle, 10x10cm^2, 15x 15 cm^2, 20 x20 cm^2 and 25 x 25cm^2 applicators.

2) Comparison of two different methods in determination of the effective source surface distance is made.

MATERIALS AND METHODS

Experimental measurements were performed in Siemens Primus linear accelerator at Department of Radiotherapy and Oncology of School of Medical Sciences. In a linear accelerator, electrons are accelerated to high energy and are allowed to exit the machine an electron beam. The linear accelerator at the HUSM produces electron beams in the energy range of 6–21 MeV. The unit has various applicators with nominal source to applicator-end-distance of 95 cm. This introduces a 5 cm air gap between the applicator end and the source axis distance (SAD).

All readings were obtained by stimulating the clinical conditions as closely as possible, that is by using solid water phantom slabs of various thicknesses as phantom materials, together with a MARKUS electron beam parallel plate ionization chamber.

A Phantom is a material with electronic density close to water and it is used to make radiation dosimetry measurement. Due to the fact that human body is made mostly of water, the best representative of the human body when interacting with radiation is water. But, to eliminate the inconvenience of transporting, setting up and filling water tanks, solid water phantoms was used to make radiation dosimetry measurement. These phantoms are usually within 0.5% of true water dosimetry. The slabs of solid water phantom used in this thesis are shown in Figure 3.

MARKUS electron beam chamber is flat and consists of a cylindrical plexiglass body whose measuring volume (5mm diameter and 2mm high) is flush to the surface. The ion chamber is energy independence with high measuring accuracy. The measuring volume of $0.05cm^3$ yields high spatial resolution, allowing the accurate determination of electron energy as well as dose distribution measurements. Parallel plate ionization chamber was used because

it has a well defined point of measurement, which is the proximal surface of the upper collecting electrode. The thin window allows measurements at the surface of a phantom without significant wall attenuation. Since the front plane of the air cavity is flat and is exposed to a uniform fluence of electrons, the effective point of measurement is the center of the sensitive air cavity of the chamber.

Charge measurements were taken by using various air gaps. Depth of measurement position is at the depth of maximum dose in electron beams, which is a function of energy and field size (Table 1). Although the effective SSD was obtained by making measurements at the depth of maximum dose, its value does not change significantly with the depth of measurement (Khan 1978). The ionization chamber was placed on 8 cm of solid water blocks for sufficient backscatter. Some of the radiation after entering the tissue will scatter back toward the surface. Extended SSD measurements were performed using optical distance indicator which projects a numerical scale onto the phantom surface to indicate source surface distance. Figure 4 and 5 show the setting for measurement.

In this method, a series of output measurements were made in a phantom at the depth of ionization charge maximum as a function of the air gap g between the end applicator and surface of the phantom. Charges collected were read out by the used of a charge measuring device- *Victoreen* Model 525 electrometer. The chamber was connected to the electrometer with a bias voltage of -200V.

Normally the photon beam collimators on the accelerator are too far from the patient to be effective for electron field shaping. After passing through the scattering foil, the electrons scatter sufficiently with the other components of the accelerator head, and in the air between exit window and the patient to create a clinically unacceptable penumbra. Electron

beam applicators or cones are usually used to collimate the beam, and are attached to the treatment unit head.

To find the effective source surface distance, measurements were performed at various SSD values ranging from 95 to 110 cm. Two different methods were used to determine the effective SSD under same experimental setup that is inverse square law method and graphical extrapolation method. The effective SSD obtained from measurements using the inverse slope and graphical extrapolation methods are found to be identical.

Measurements were carried out first with the applicator in contact with the phantom and then with an increasing air gap of 5, 10, and 15 cm between the applicator end and the phantom. Measurements of the charge were performed at varying distances of the phantom surface from the plane perpendicular to the beam axis at the isocentre, which is the normal treatment position where g is the gap distance from the end of applicator to the phantom surface, Q_0 is the ionization charge reading at d_{max} at standard nominal SSD (95cm) and Q_g is the reading with gap g, for extended SSDs. By plotting $[Q_o/Q_g]^{½}$ as a function of g, a straight line was obtained having slope $1/(SSD_{eff} + d_{max})$. The effective SSD is then equal to $SSD_{eff} = (1/slope)-d_{max}$. The slope of the graph plotted from this equation was determined by using simple linear regression equation.

Graphical extrapolation is the process of reading values from a graph outside the range of the actual data points. Curves were plotted between the inverse of the square of the charge due to ionization against air gap, and by graphical extrapolation on the graph paper, effective SSD could be determined.

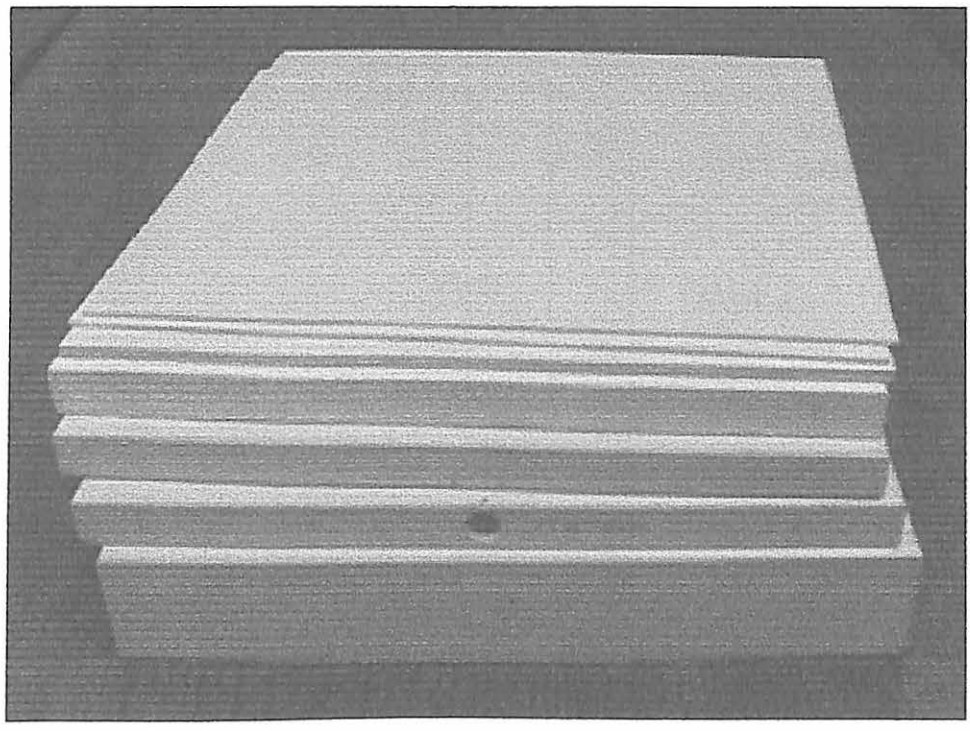

Figure 3. 30cm x 30 cm slabs of solid water phantom

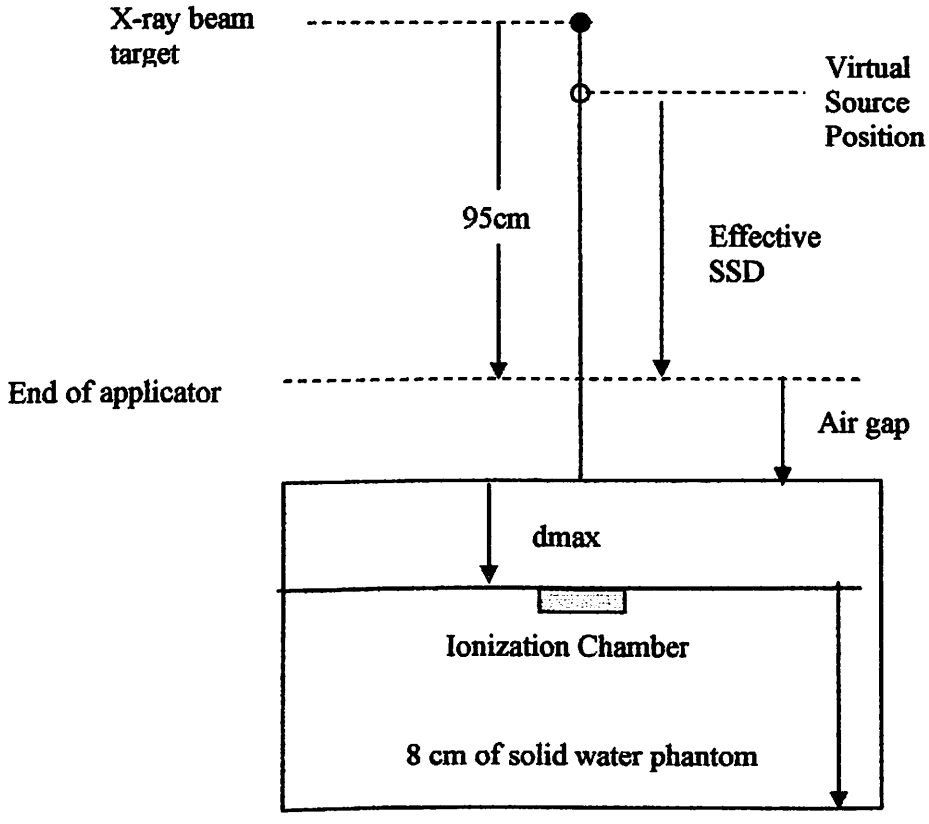

Figure 4. The experiment set up showing the virtual source position, effective SSD, air gap and depth of measurement.

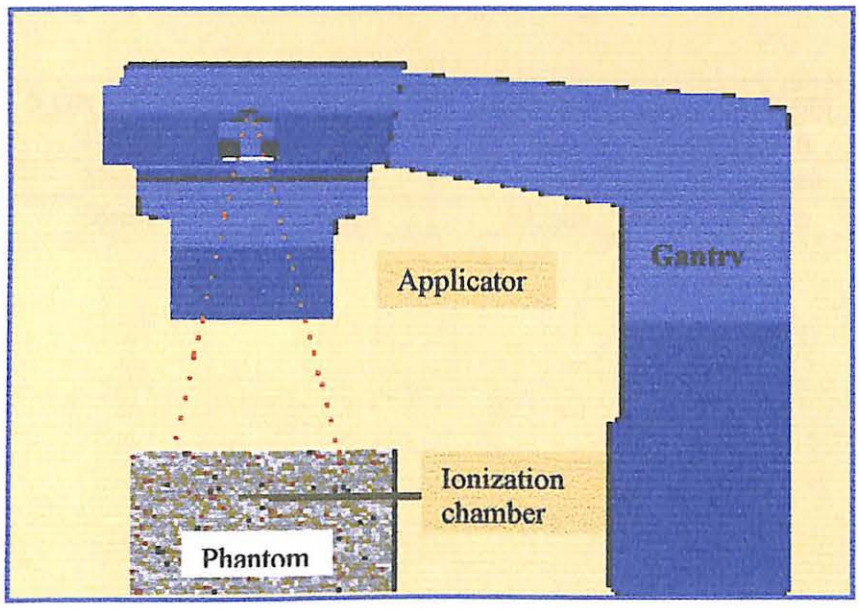

Figure 5. Linac and solid water phantom setup

Table 1: Depth of maximum dose as a function of energy and field size.

Energy	5 cm dia.cicle	10 x10 cm^2	15 x 15cm^2	20 x 20cm^2	25 x 25cm^2
6	14mm	14mm	14mm	14mm	14mm
9	20mm	20mm	21mm	21.5mm	21mm
15	16mm	18mm	14mm	14mm	12mm

RESULTS

Table 2, 4 and 6 present the square root of the ratio of ionization charges, $[Q_o/Q_g]^{1/2}$ with 5 cm diameter circle applicator for 6, 9, and 15 MeV respectively. For a fixed energy and applicator, the values of $[Q_o/Q_g]^{1/2}$ increases with air gap.

Table 3 present the calculated data to obtain the slope for 5 cm diameter circle applicator in 6 MeV electron beam energy. The slope was simply calculated by dividing 2.0925 with 125, namely 0.016743. The depth of maximum dose, d_{max} at this measurement condition is 1.4cm, shown in table 1, thus the effective SSD is then equal to $(0.01673)^{-1}$-1.4. The effective SSD is 58.3 cm.

The slope of the calculated data in table 5 for 5 cm diameter circle applicator in 9 MeV electron beam energy was determined by dividing 1.79325 with 125, namely 0.014346. The depth of maximum dose, d_{max} at this measurement condition is 20mm, thus the effective SSD is then equal to $(0.014346)^{-1}$-2.0cm. The effective SSD is 67.7cm

The slope of the calculated data in table 7 for 5 cm diameter circle applicator in 15MeV was calculated by dividing 1.7825 with 125, namely 0.01426. The depth of maximum dose, d_{max} at this measurement condition is 16mm, thus the effective SSD is then equal to $(0.01426)^{-1}$-1.6cm. The effective SSD is 68.5cm.

Table 8, 10 and 12 present the square root of the ratio of the ionization charge, $[Q_o/Q_g]^{1/2}$ with 10 cm x 10 cm applicator for 6, 9, and 15 MeV respectively. For a fixed energy and applicator, the values of $[Q_o/Q_g]^{1/2}$ also increases with air gap.

Table 9 present the calculated data to obtain the slope for 10 cm x 10 cm applicator in 6 MeV electron beam energy. The slope was simply calculated by dividing 1.51 with 125,

namely 0.01208. The depth of maximum dose, d_{max} at this measurement condition is 14mm, thus the effective SSD is then equal to $(0.01208)^{-1}$-1.4cm. The effective SSD is 81.4cm.

Table 11 present the calculated data to obtain the slope for 10 cm x 10 cm applicator in 9 MeV electron beam energy. The slope was simply calculated by dividing 1.435 with 125, namely 0.01148. The depth of maximum dose, d_{max} at this measurement condition is 20mm, thus the effective SSD is then equal to $(0.01148)^{-1}$-2.0cm. The effective SSD is 85.1cm

Table 13 present the calculated data to obtain the slope for 10 cm x 10 cm applicator in 15 MeV electron beam energy. The slope was simply calculated by dividing 1.3725 with 125, namely 0.01098. The depth of maximum dose, d_{max} at this measurement condition is 18mm, thus the effective SSD is then equal to $(0.01098)^{-1}$-1.8cm. The effective SSD is 89.3cm

Table 14, 16 and 18 present the square root of the ratio of the ionization charge, $[Q_o/Q_g]^{1/2}$ with 15 cm x 15 cm applicator for 6, 9, and 15 MeV respectively. For a fixed energy and applicator, the values of $[Q_o/Q_g]^{1/2}$ increases with air gap.

Table 15 present the calculated data to obtain the slope for 15 cm x 15 cm applicator in 6 MeV electron beam energy. The slope was simply calculated by dividing 1.355 with 125, namely 0.01084. The depth of maximum dose, d_{max} at this measurement condition is 14mm, thus the effective SSD is then equal to $(0.01084)^{-1}$-1.4cm. The effective SSD is 90.9cm.

Table 17 present the calculated data to obtain the slope for 15 cm x 15 cm applicator in 9 MeV electron beam energy. The slope was simply calculated by divided 1.3425 with 125, namely 0.01074. The depth of maximum dose, d_{max} at this measurement condition is 21mm, thus the effective SSD is then equal to $(0.01074)^{-1}$-2.1cm. The effective SSD is 91cm.

Table 19 present the calculated data to obtain the slope for 15 cm x 15 cm applicator in 15 MeV electron beam energy. The slope was simply calculated by dividing 1.3225 with 125, namely 0.01058. The depth of maximum dose, d_{max} at this measurement condition is 14mm, thus the effective SSD is then equal to $(0.01058)^{-1}$-1.4cm. The effective SSD is 93.1cm

Table 20, 22 and 24 present the inverse square root of the ratio of the ionization charge, $[Q_o/Q_g]^{1/2}$ with 20 cm x 20 cm applicator for 6, 9, and 15 MeV respectively. For a fixed energy and applicator, the values of $[Q_o/Q_g]^{1/2}$ increases with air gap.

Table 21 present the calculated data to obtain the slope for 20 cm x 20 cm applicator in 6 MeV electron beam energy. The slope was simply calculated by dividing 1.245 with 125, namely 0.00996. The depth of maximum dose, d_{max} at this measurement condition is 14m, thus the effective SSD is then equal to $(0.00996)^{-1}$-1.4cm. The effective SSD is 99.6cm.

Table 23 present the calculated data to obtain the slope for 20 cm x 20 cm applicator in 9 MeV electron beam energy. The slope was calculated by divided 1.255 with 125, namely 0.01004. The depth of maximum dose, d_{max} at this measurement condition is 21.5mm, thus the effective SSD is equal to $(0.01004)^{-1}$-2.15cm. The effective SSD is 97.4cm.

Table 25 present the calculated data to obtain the slope for 20 cm x 20 cm applicator in 15 MeV electron beam energy. The slope was simply calculated by dividing 1.21 with 125, namely 0.00968. The depth of maximum dose, d_{max} at this measurement condition is 14mm, thus the effective SSD is then equal to $(0.00968)^{-1}$-1.4cm. The effective SSD is 101.9cm.

Table 26, 28 and 30 present the inverse square root of the ratio of the ionization charge, $[Q_o/Q_g]^{1/2}$ with 25 cm x 25 cm applicator for 6, 9, and 15 MeV respectively. For a fixed energy and applicator, the values of $[Q_o/Q_g]^{1/2}$ increases with air gap.

Table 27 present the calculated data to obtain the slope for 25 cm x 25 cm applicator in 6 MeV electron beam energy. The slope was simply calculated by dividing 1.255 with 125, namely 0.01004. The depth of maximum dose, d_{max} at this measurement condition is 14mm, thus the effective SSD is then equal to $(0.01004)^{-1}$-1.4cm. The effective SSD is 98.2cm.

Table 29 present the calculated data to obtain the slope for 25 cm x 25 cm applicator in 9 MeV electron beam energy. The slope was simply calculated by dividing 1.2975 with 125, namely 0.01038. The depth of maximum dose, d_{max} at this measurement condition is 21mm, thus the effective SSD is then equal to $(0.01038)^{-1}$-2.1cm. The effective SSD is 94.2cm

Table 31 present the calculated data to obtain the slope for 25 cm x 25 cm applicator in 15 MeV electron beam energy. The slope was simply calculated by dividing 1.165 with 125, namely 0.00932. The depth of maximum dose, d_{max} at this measurement condition is 12mm, thus the effective SSD is then equal to $(0.00932)^{-1}$-1.2cm. The effective SSD is 105.9cm.

Figure 6-10 present $[Q_0/Q_g]^{1/2}$ as a function of the air gap introduced between the nominal and extended SSD for all available applicators. The measured data follow a straight line for each electron energy; however, the slopes of the lines are different leading to different effective SSDs for different electron beams defined by the various applicators.

Table 32 presents the dependence of effective SSD on incident energy and field size. Effective SSD showed a slight increase with energy. The effective SSD for a given energy is small for smaller field sizes, and increases with field size.

Plotted of the calculated effective SSD against the energy of measurement, showed that the effective SSD varied with beam energy. Figure 11 illustrates this variation for a range

of electron energies obtained for all available applicators. The effective SSD increases with energy to a maximum value. The higher energy beams reached effective SSD values of 106 for larger field sizes. The minimum effective SSD is found in the 6 MeV with 5 cm diameter circle applicator that is 58.3 cm.

Figure 12 shows the variation in effective SSD with field size. The effective SSD increased with increasing field size and was seen more clearly with the lower energy electrons, 6 MeV. After the maximum values, the effective SSD value decreased by 1.4 cm and 3.2 cm for the 6 MeV and 9 MeV respectively, after 20 cm x 20 cm applicator. For larger field sizes, the effective SSD appears to deviate less from the nominal value of 95 cm.

The effective SSDs determined by with two different measurement methods, namely inverse slope method and graphical extrapolation method are given in table 33. The effective SSD increased from 58.3 cm for beam energy of 6 MeV to a maximum of 106.1 cm for beam energy of 15 MeV. The effective SSDs for 9 MeV were found to be less than that for 6 MeV beams, for 20 cm x 20 cm and 25 cm x 25 cm applicator. The effective SSDs obtained from the graphical extrapolation increased with the increase in electron energy and field size, except for 9 MeV with 15 cm x 15cm, 20 cm x 20 cm and 25 cm x 25 cm applicators.

The effective SSD obtained by graphical extrapolation for all available applicators for 6, 9 and 15 MeV are shown in figure 13-27.

The variation of the effective SSD determined by inverse slope method and graphical extrapolation are listed in table 34, which varied from 0.981 to 1.012.

Table 2: Measured data for 6 MeV electron energy; 5 cm diameter circle

SSD, cm	Gap, cm	Ionization Charge, nC			$[Q_o/Q_g]^{1/2}$
		First Reading	Second Reading	Mean Reading	
95	0	1.617	1.621	1.619	1.000
100	5	1.408	1.405	1.409	1.080
105	10	1.212	1.211	1.212	1.164
110	15	1.028	1.039	1.033	1.251

Table 3: Calculation of the total sum of squares, Sxx and Sxy

x	y	$x-\bar{x}$	$y-\hat{y}$	$(x-\bar{x})^2$	$(x-\bar{x})(y-\hat{y})$
0	1.000	-7.5	-0.1238	56.25	0.9285
5	1.080	-2.5	-0.0438	6.25	0.1095
10	1.164	2.5	0.0402	6.25	0.1005
15	1.251	7.5	0.1272	56.25	0.9540
$\bar{x} = 7.5$	$\hat{y}= 1.1238$			$\Sigma (x-\bar{x})^2 = 125$	$\Sigma(x-\bar{x})(y-\hat{y})=$ 2.0925

Table 4: Measured data for 9 MeV electron energy; 5 cm diameter circle

SSD, cm	Gap, cm	Ionization Charge, nC			$[Q_o/Q_g]^{1/2}$
		First Reading	Second Reading	Mean Reading	
95	0	1.952	1.959	1.956	1.000
100	5	1.698	1.694	1.696	1.074
105	10	1.493	1.499	1.496	1.143
110	15	1.323	1.322	1.322	1.216

Table 5: Calculation of the total sum of square, Sxx and Sxy

x	y	$x-\bar{x}$	$y-\hat{y}$	$(x-\bar{x})^2$	$(x-\bar{x})(y-\hat{y})$
0	1.000	-7.5	-0.1083	56.25	0.81225
5	1.074	-2.5	-0.0343	6.25	0.08575
10	1.143	2.5	0.0347	6.25	0.08675
15	1.216	7.5	0.1078	56.25	0.80850
$\bar{x} = 7.5$	$\hat{y}= 1.1083$			$\Sigma (x-\bar{x})^2 = 125$	$\Sigma(x-\bar{x})(y-\hat{y})=$ 1.79325

Table 6: Measured data for 15 MeV electron energy; 5 cm diameter circle

SSD, cm	Gap, cm	Ionization Charge, nC			$[Q_o/Q_g]^{1/2}$
		First Reading	Second Reading	Mean Reading	
95	0	2.159	2.152	2.155	1.000
100	5	1.842	1.849	1.845	1.071
105	10	1.638	1.635	1.637	1.145
110	15	1.462	1.461	1.462	1.213